Marine climate change over the eastern Agulhas Bank of South Africa

Mark R Jury
Geography Dept, University of Zululand, KwaDlangezwa 3886, South Africa
and Physics Dept., University of Puerto Rico Mayaguez, USA, 00681
re-submitted to EGU ocean Sci Oct~~4 June~~ 2020

Abstract

The rate of change in the marine environment over the eastern Agulhas Bank, along the south coast of South Africa (32-37S, 20-30E) is studied using reanalysis observations 1900-2015 and coupled ensemble model projections 1980-2100. Outcomes are influenced by resolution and time-span: ~1 degree datasets covering the whole period capture large-scale changes, while ~0.5 degree datasets in the satellite era better distinguish the cross-shelf gradients. Although sea surface temperatures offshore are warming rapidly (.05°C/yr since 1980), a trend toward easterly winds and a locally stronger Agulhas Current have intensified near-shore upwelling (-.03°C/yr). The sub-tropical ridge is gradually moving ~~during summer is drawn~~ poleward, leading to a ~~by global warming and high phase southern oscillation index. Cooler inshore sea temperatures suppress latent heat flux and contribute to coastal desiccation (-.005 mm day^{-1}/yr) and vegetation warming (.1°C/yr) since 1980. Coupled ensemble projections from the Hadley and European models indicate that the shift toward~~ drier climate~~weather and easterly winds may be sustained through the 21st century~~.

Key words: South African, coastal climate change
mark.jury@upr.edu

Introduction

The marine climate of the eastern Agulhas Bank along the south coast of South Africa is shaped by the continental plateau and sub-tropical latitude. Rainfall tends to be limited and shelf waters are characterized by sharp gradients between inshore upwelling and an offshore current that advects warm water polewards at ~1 m/s (Lutjeharms et al. 2000). Downstream widening of the shelf and cyclonic shear causes uplift at the shelf edge (Schumann et al. 1982, Lutjeharms 2006, Goschen et al. 2015, Malan et al. 2018). Westerly and easterly wind regimes during winter to summer respectively induce alternating spells of downwelling and upwelling (Schumann and Martin 1991, Schumann 1999). Numerous small rivers discharge into the shelf zone (Schumann and Pearce 1997, Scharler and Baird 2005, vanBladeren et al. 2007). The inshore environment and large embayments (Fig 1a) are characterized by weak circulations and seasonal warming, and become stratified and productive during austral summer (Roberts 2010, Pattrick et al. 2013). The Agulhas Current meanders a few times per year (Goschen and Schumann 1990, Rouault and Penven 2011), while the mid-latitude jet stream meanders a few times per month advecting coastal lows and continental shelf waves along the shelf (Jury et al. 1990, Schumann and Brink 1990). Amidst these rapid changes are rising sea levels (Mather et al. 2009~~; Jury 2018~~) and longer summers.

The eastern Agulhas Bank shows trends toward offshore warming and inshore cooling due to wind- and current-induced upwelling, and retreat of the circumpolar westerlies (Rouault et al. 2009, Durgadoo et al. 2013, Hutchinson et al. 2018). Trends in air temperatures are near the global average ~~Past research has found trends~~ of .02°C/yr (Kruger and Shongwe 2004, Morishima and Akasaka 2010, Jury 2013), but~~however~~ trends in other variables show multi-year fluctuations (Philippon et al. 2012) from ~~tend to be over-shadowed by~~ regional atmosphere coupling with sea surface temperatures (SST) and the Pacific El Niño Southern Oscillation (ENSO). Climate change~~short-term~~ analyses of ~~events and the sparsity of data before 1950 (~~Tadross et al. (2005), MacKellar et al. (2014) and~~,~~ Kruger and Nxumalo (2017) offer guidance on ~~-~~resource management, which this research seeks to extend.

The main objective of this study~~research~~ is to establish the rate and pattern of observed and projected marine climate (land, air, sea) trends along the south coast of South Africa from 1900 to 2100. Scientific questions include: 1) How has the wind field responded to a poleward shift of the subtropical ridge~~, and how does that affect the shelf temperature and currents~~? 2) What are the consequences of intensified ~~If the~~ coastal ~~ocean is cooling due to wind- and current-driven~~ upwelling~~, in contrast with the offshore environment – what are the consequences for the local heat and water budget~~? 3) How does record length and dataset resolution affect the result? and 4) W~~w~~hat is the impact of climate variability ~~(eg. El Niño Southern Oscillation, ENSO)~~ on trend attribution? While the spatial focus is on the south coast of South Africa using monthly datasets finer than 0.5° during the satellite era, context is provided at the large-scale using coarser model products over the 20th and 21st centuries.

Formatiert: Hochgestellt

Formatiert: Hochgestellt

Data and Methods~~ology~~

Modern data assimilation systems blend in-situ and ancillary measurements by iterating between climatology, persistence and theory, interpolating across gaps in time and space, and limiting the influence of outliers. By reducing uncertainties, scientists now have a reliable means to evaluate trends in marine climate. The monthly reanalysis products employed here include: ECMWFv5~~-int atmosphere~~ coupled (Dee et al. 2011), ECMWF-20c atmosphere (Poli et al. 2016), ECMWF-ora4 ocean (Balmaseda et al. 2013), NASA MERRA-2 coupled~~atmosphere~~ (Gelaro et al. 2017), NCEP CFSr-2 coupled (Saha et al. 2010), SODA-3 ocean (Carton et al. 2018), NOAA sea surface temperature (SST; Reynolds et al. 2007), NOAA net outgoing longwave radiation (OLR; Lee et al. 2007), ~~and~~ NESDIS vegetation temperature (Tucker et al., 2005), and CHIRP rainfall (Funk et al. 2014). Table 1 lists the acronyms, data source, horizontal resolution and time-span. Ocean-atmosphere fields with horizontal resolution finer than 0.5°~~50 km~~ are capable of representing cross-shelf gradients, and these are available in the satellite era 1980-2016~~5~~. SODA-3 provides sub-surface ocean data on temperature, salinity, currents and vertical motion; driven by MERRA-2 winds, multi-satellite altimeter and thermal measurements, blended with in-situ observations over the shelf. L~~Coupled l~~and-atmosphere-ocean evolution is described by coupled reanalysis ~~ECMWF~~ products underpinned by data assimilation (Hamrud et al 2015).

In addition to the monthly datasets, daily ECMWF-5~~int~~ sea level air pressure (SLP) fields were analyzed using ~~transient~~ empirical orthogonal functions (EOF). The leading mode was determined and its spatial loading pattern and time score were analyzed for evolution at lags from -2 to +2 days, and for trends and spectral cycling in~~over~~ the period 1900-2015. Ship data, from the repository for marine data collected in South African waters: SADCO, were analyzed in 0.1° bins for SST and wind speed, averaged 24.5-26.5°E 1950-2015 (cf. Fig A1) and compared with 0.3° reanalysis products. Monthly river discharge records were obtained for the Gamtoos and Sundays Rivers from the SA Department of Water Affairs hydrology service: SADW, and combined to understand the coastal hydrology.

Bias was examined via inter-comparisons between SADCO SST and wind speed, and the satellite-era reanalyses (CFSr-2, ECMWF-5, MERRA-2). These show coherent cross-shelf gradients (cf. Fig A1) indicating they capture the inshore upwelling. The reanalyses diverge at the coast, depending on resolution and land-sea ratio.

The statistical method used to ~~for~~ quantify~~analyzing~~ marine climate change is linear~~to~~ regression- of a trend line over a long record of temporal data, using the Pearson Product Moment least squares technique. The resultant slope and r^2 fit of the regression line provides a statistical way of determining the rate of change or trend (signal) within the inter-annual fluctuations (noise). The temporal data are filtered to annual and area-averages, according to the insights required.

Linear trends are spatially analyzed per grid point in three domains: large-scale map 45°-20°S, 10°-50°E, regional-scale map: 32-37°S, 20-30°E, and depth sections over the shelf: 37-33°S, averaged 24.5-26.5°E. Local trends are calculated by regression onto time series averaged over the index area (35.5-33.5°S, 24.5-26.5°E, Fig 1a) after reduction to annual and seasonal (Dec-Feb) averages~~interval~~. For example, a sea temperature warming of 3°C over 100 years yields a .03 C/yr slope which is mapped in relation to adjacent regression-fitted slopes. If year-to-year fluctuations reduce the r^2 fit below a certain statistical threshold, then it is inferred that the signal is swamped by noise. Trends for U, V, W wind and current components are calculated separately and combined into 'trend' vectors that represent the slope or rate of change, as maps and sections. The r^2 fit of the trend is evaluated for significance at 95% confidence. For long-term records having > 100 degrees of freedom, a meaningful outcome requires $r^2 > 4\%$ ($r > |0.2|$). For satellite era records having < 40 degrees of freedom, thresholds are reached at $r^2 > 9\%$ ($r > |0.3|$). Trends are embedded in noisy marine environments, and so depend on time-span, local climate variability (Schlegel and Smit 2016), and quality of the input data (Chaudhuri et al. 2013). The CFSr-2, ECMWF~~-int~~, and MERRA-2 reanalyses exhibit similar trends (Kennedy et al. 2011, Decker et al. 2012) and yield comparable turbulent fluxes around South Africa (Nkwinkwa et al. 2019).

The trend of SST and zonal winds are analyzed by correlating the slope against its time series, for each month. For most variables ~~zonal winds,~~ the index area is; ~~used (~~ 35.5-33.5°S, 24.5-26.5°E (Fig 1a); ~~, but~~ for SST the ~~analysis distinguishes between~~ coast ~~(33.8-33~~(33.8~~.9~~°S) and shelf-edge (~~34.9~~ 35.0~~.0~~°S) are distinguished~~latitude bands~~. The resultant correlation values per month are plotted over the annual cycle to detect the seasonality of trends in the period 1980-2015.

Using 18-month filtered values, hovmoller plots were constructed across the shelf to identify how intra-decadal fluctuations mingle with climate change signals. After exploratory statistical tests, a modulating influence was attributed to the Pacific southern oscillation index (SOI) or east-west difference in SLP. Its time score is analyzed for trend and correlated with local SST and zonal winds in annual and seasonal intervals 1980-2015. Similarly, a dipole mode is extracted by EOF analysis of filtered ECMWF-esm projected SLP fields in the tropical Pacific, and temporal characteristics are studied.

Projections of air temperature, precipitation and zonal winds from the coupled ensemble ECMWF-esm v2.3 model (Taylor et al. 2012, Doblas-Reyes et al 2018) are analyzed over 1980-2100 as large-scale trend maps and index-area time series. The simulation is forced by the rcp8.5 greenhouse scenario (vanVuuren et al. 2011, CO_2 +5 ppm/yr), and incorporates data assimilation in the first 35 years that overlap with observations. Like most long-term projections, intra-member dispersion is constrained by ensemble averaging and trends therefore emerge. The coupled ensemble Hadley-esm model (Collins et al. 2011) is analyzed for zonal currents in the 0-50 m layer. Prior research found that this model is one of the few to realistically represent ocean ‘dynamic topography’ ~~(Jury 2018)~~ and sea level pressure fields around southern Africa (Dieppois et al. 2015). Its mean annual cycle of zonal currents closely follows the reference Aviso-Copernicus product (cf. Fig A2).

An intercomparison of in-situ measurements, reanalysis fields and model simulations is covered in the Appendices; the above references provide insight on global validations. SADC s~~S~~hip SST and wind speed data averaged in~~sliced in~~ 0.1 deg~~10 km~~ intervals~~s~~ describe the cross-shelf gradient in Figure A1, compared with reanalysis at native resolution. The coarser long-term model and reanalysis products (cf. Table 1) under-represent ~~the~~ inshore upwelling, so~~and~~ outcomes are ~~thus~~ restricted to large-scale winds and rainfall. Annual cycle inter-comparisons of index-area SST and zonal wind 1980-2015 are given in Figure A2, and suggest that model seasonality is ~10% greater than observed. In Figure A3, context is provided on regional SOI influence.

Results

Study area and large-scale trend maps

The study area is illustrated in Fig 1a, and shows steep topographic and bathymetric gradients, with >1000 m mountains in latitudes < 33ºS, the coast at 34ºS, shelf-edge at 35ºS and deep ocean to the south. The coastline is convex and indented by two bays and associated capes; the continental slope steepens eastward. The vegetation trend map (Fig 1b) reflects a warming rate of

.1ºC/yr since 1980 that increases northwest inland in conjunction with potential evaporation losses (-.005 mm day^{-1}/yr). Coastal cities of Port Elizabeth and East London have slower rates of warming. The coarse-scale ECMWF-20c trend maps for SST and zonal wind (Fig 1c,d) reveal a warming .02ºC/yr in the Agulhas Current retroflection and reduced values in the sub-tropical zones where easterly winds are accelerating over 1900-2010 (U = -.01 m s^{-1}/yr), consistent with Dlomo (2014). Easterly winds have accelerated in the south Atlantic and south Indian anticyclones and over the interior of southern Africa, but in the southern mid-latitudes a westerly trend is noted over the 20th century.

The ECMWF-20c trend map for precipitation minus evaporation (Fig 1e) indicates a growing deficit in the Mozambique Channel, the source region of the Agulhas Current (Fig 1f). Weaker deficits are noted over the South Atlantic, while weak surplus trends are found over the eastern highlands of South Africa and in the South Indian Ocean mid-latitudes. The shelf-edge Agulhas Current converges and accelerates just east of the study area, then fans out and retroflects (Lutjeharms 2006).

Regional ocean trend maps and sections

The NOAA SST trend map shows warming >~-.05°C/yr along the shelf edge 1981-2016 (Fig 2a) similar to Rouault et al. (2010), and . Yet inshore there is a distinct cooling trend that is faster in Algoa Bay than elsewhere (-.03°C/yr inshore). Trends in SODA-3 salinity are weakly positive along the coast in the period 1980-2015, suggesting reduced river run-off and greater evaporation. Surface layer flow is accelerating in the shelf-edge Agulhas Current, particularly downstream from the study area (Fig 2c). Outside the current, a pair of gyres (36°S, 25° & 29°E) directs flow toward the coast. This onshore pattern has little context and may be set aside until confirmed elsewhere.

SODA-3 depth section trends (Fig 2d,e,f) show that the warming trend at the shelf edge is aligned with a locally n accelerating Agulhas Current (U = -.006 m s^{-1}/yr at 35.3°S; Backeberg et al.

2012). The cooling trend along the coast is confined to a shallow layer < 40 m, and would accentuate the $\partial\eta/\partial y$ gradient. Trends in the meridional circulation reveal upwelling at depth and offshore transport in the near-shore zone. There is a sharp transition to downwelling and onshore transport seaward of 35.6°S. Taken together the trend is for convergence onto the Agulhas Current and faster downstream advection at the shelf edge. Trends ~~Changes~~ in the Agulhas Current are relatively uniform over depth (cf. Fig 2e), suggesting ~~exhibit little vertical shear,~~ that ~~consequently~~ cyclonic vorticity-induced uplift is locally ~~uniformly available but~~ concentrated by ~~the~~ shelf slope (cf. Fig 2f)~~(Lutjeharms 2006)~~.

Regional wind and pressure trends

Trend maps are illustrated for reanalysis winds and latent heat flux in Fig 3a,b. Winds show a distinct shift toward easterly winds 1980-2015, linking the South Atlantic and South Indian anticyclones. The wind trends follow the convex coastline and divide zones of rising and falling latent heat flux, consistent with the SST trends (cf. Fig 2a). A trend toward northeasterly winds and ~~The~~ reduced moisture flux over land~~in the terrestrial environment~~ promotes hydrological deficit.

Regional atmospheric circulation trends were studied via EOF analysis of Dec-Feb daily SLP data. This helps place the transient weather into long-term context. Mode-1 accounts for 38% of variance (Fig 3c,d). Its loading pattern shows a mid-latitude antityclone passing eastward over a 5-day period, followed by a trough along the west coast that subsequently spawns a coastal low. The mode-1 time score shows fluctuations within an upward trend (slope = .008 hPa/yr, r^2 = 11%), indicating more frequent anticyclonic ridging. The gradual poleward shift of the subtropical wind belt is comprized of pulsed synoptic weather.

Shelf analysis and gradients

Hovmoller plots were constructed across the southern shelf (Fig 4a-d~~,b~~) for 18-month filtered SST~~surface temperature,~~ ~~and~~ zonal winds / currents / vertical motion, and rainfall. There is a multi-year alternation of warm and cool ~~. Warm~~ spells ~~during westerly wind-driven downwelling~~

~~contrast with cool spells during easterly wind-driven upwelling: a multi-year alternation~~, modulated by local winds and the Pacific El Nino / La Nina (Jury 2015, 2019) and the Southern Annular Mode (Malan et al. 2019). T~~Yet t~~here is a background trend of~~toward~~ inshore cooling and offshore warming that intensifies the coastal gradient (Fig 4a).~~.~~ The SST pattern is supported by Ekman transport from inshore easterlies and offshore westerlies - that pulse in 1992 and 2013 (Fig 4b). Rainfall (Fig 4c) displays a sharp boundary at 34.5°S between dry inshore / wet offshore climates. Coastal upwelling and atmospheric subsidence suppress moist convection, whereas the Agulhas Current enhances marine rainfall ~ 3-fold. The sharp change in CHIRP rainfall regime on 34.5°S coincides with accelerated longshore winds. The hovmoller plot of SODA-3 near-surface zonal currents (Fig 4d~~b~~) reveals pulsed intensification and coastward shift, contributing to near-shore uplift > 4 m/day (34.1-34.4°S). C~~Thus c~~urrent- and wind-induced upwelling appear additive much of the time. However in 2013 currents prevailed over winds, suggesting occassional decoupling.

Index-area time series of reanalysis and projected near-surface zonal currents (Fig 4c) show a trend of local ~~n~~ acceleration~~ng tendency~~. Past and future linear regression slopes are -.0076 m s^{-1}/yr, with trend correlations rising from -.81 to -.90. Future (2nd order) trends overlie those from past reanalysis and year-to-year fluctuations are consistent despite technology artifacts of satellite altimetry and ensemble averaging. Appendix A2 compares the index-area annual cycle of model vs observation. This index-area covers much of the Agulhas Current in longitudes where the shelf is convex (cf. Figs 1a, 2e).

The trend of NOAA SST analyzed in coastal and shelf-edge latitudes show contrasting values but little change over the annual cycle in Fig 5a. Shelf-edge waters are warming steadily (r= +.5) while coastal waters are cooling (r= -.5)~~, slightly~~ moreso from February to May (slope -.04°C/yr). Together these indicate a tightening gradient ($\partial T/\partial y$) and a steepening sea slope. The annual cycle of index-area zonal wind trends (Fig 5b), averaged over three reanalyses, reveals that easterly winds are intensifying during summer (Nov-Feb), when subtropical ridging is most likely.

Regression of SST and winds onto the southern oscillation index (Fig 5c,d) reveals trend patterns similar to climate change: inshore cooling (mainly summer) and offshore warming (all-year). Winds with respect to high-phase SOI are from northeasterly and considerably stronger in summer, hence wind-driven coastal upwelling is favoured during La Nina. The southern oscillation index has shown an upward trend during the satellite era, and its regression onto regional sea level air pressure patterns (cf. Fig A3) matches the earlier mode-1 pattern of mid-latitude high / sub-tropical low (cf. Fig 3c). Hence l~~L~~ong-term and multi-decadal trends tend to conspire~~are acknowl-edged to be additive here~~.

Hydrology trends

The ~~earlier discovery of~~ increasing near-shore salinity (cf. Fig 2b) could be ~~was~~ related to drying trends in the adjacent terrestrial climate~~, supported by declining latent heat flux~~ (cf. Fig 3b). In Fig 5e the regional hydrology is studied using the combined Gamtoos and Sundays River discharge record. Although flood / drought events and 2-5 yr cycles are evident, there is ~~no appreciable~~ little trend. The study area lies between a zone of reduced cloudiness (Benguela – Namib) to the northwest and increased cloudiness to the southeast, as seen in the trend map for satellite net OLR (Fig 5f). The rising ~~Increasing~~ salinity off~~along~~ the south coast (cf. Fig 2b) may be attributed ~~scribed~~ to advection from the Mozambique Channel, where evaporation exceeds precipitation (cf. Fig 1e). Vertical motions over the shelf could also play a role (cf. Fig 2f), whereby cyclonic shear lifts salty water.

Model projections under greenhouse warming

Spatial maps of ECWMF-esm rcp8.5 trends for zonal wind and rainfall 1980-2100 show a key feature southeast of the study area (Fig 6a,b). Easterly winds are projected to increase and rainfall is expected to decrease. The warm moist air carried westward beneath a stable inversion layer generates less evaporation, so rain-bearing storms are projected to diminish in strength and be deflected poleward by the sub-tropical anticyclone.

Time series of index-area values comparing ECMWF-20c reanalysis with ECMWF-esm and Hadley-esm projections are given in Fig 6c-f. Coupled ensemble values overlie the observation-based product indicating little bias but lower variance. Zonal winds that oscillate in a stationary manner through the 20^{th} century tend toward easterly (-U) in conjunction with declining precipitation. Air temperatures show a gradual rise during the 20^{th} century in both reanalysis and overlapping simulation. Thereafter, the warming trend steepens due to the greenhouse scenario. There appears to be little moderating influence of cooler nearshore SST, which coarse resolution products under-represent (cf. Fig 1c). The SOI time series is relatively stationary, but larger amplitude swings are noted in the early 20^{th} and late 21^{st} century. High phase (Pacific La Nina) events seem steady but El Nino events appear to deepen after 2040. In summary, past zonal winds of 1 m/s (after cancellation of east-west components) are projected to reach -1 m/s by 2050. Past rainfall of 1.5 mm/day declines below 1 mm/day, and air temperatures of 17°C rise above 20°C by 2050. The regression r^2 fit of trends are in the range from 72-97% and suggest sustained changes for temperature, however wind and rain tend to oscillate in the ECMWF-esm projection until the rcp8.5 scenario prevails.

In addition to ENSO influence, the Southern Annular Mode (SAM) plays a role in the latitude and intensity of basin-scale anticyclonic gyres that support the Agulhas Current (Yang et al. 2016; Elipot and Beal 2018). The long-term trend in the SAM is a contraction of circumpolar westerlies that enables poleward expansion of the tropical Hadley circulation and belt of easterly winds rounding the tip of Africa seen here (cf. Fig 3a, 6a). Yet SAM trends are flattening with recovery of the Antarctic ozone hole (Arblaster et al. 2011), and may exert less effect in future.

Discussion and summary

This study addressed a range of questions around spatial patterns in trends and uncovered evidence of a pulsed poleward shift of the subtropical ridge (cf. Fig 3c,d). Analysis of land-atmosphere-ocean conditions revealed intensified coastal upwelling from increased easterly winds. A steeper ∂T/∂y produces a~~a~~ locally faster shelf-edge current, with consequences for ~~and~~ current-induced upwelling (Schumann & Beekman 1984, Swart & Largier 1987) and increased easterly wind, with consequences for coastal dessication. Employing coupled reanalysis and model projections to distinguish coast and offshore features, a unifying patternprocess emergedwas found: summer-time wind-driven upwelling enhances geostrophic gradients and the Agulhas Current. Although ocean reanalysis outcomes are moving toward The technology is reaching consensus based on a shared data assimilation system, yet interpretations need not favour one process over another: wind vs current, fluxes vs advection, multi-decadal vs trend, local vs remote. Multi-variate forcing is We do not expected one-dimensional answers.

To place these results in context, trends in global coastal SST were analyzed over the satellite eraaround the world (not shown). Coastal upwelling zones show cooling < -.03°C/yr: broadly off SW Africa (Namibia) 35-20S, NW Africa (Sahara) 15-30N, SW America (Peru 5-25S and California 30-40°N, and narrowly off Somalia 10-15N, Namibia 35-20°S and Western Sahara 15-30°N. Even shelf waters of the USA Carolinas 30-40°N are cooling and, like the south coast of South Africa, there is a warm current offshore. Steeper gradients could produce faster shelf-edge flow, but the Gulf Stream is decelerating (Jury 2020) unlike the Agulhas Current. Figures 2c and 4de gave evidence of locally a significant increasinge in westward currents off Cape St Francis (35.5-33.5°S, 24.5-26.5°E) in using low resolution ocean reanalysis and coupled model projections. Perhaps wind-driven eddies are broadening the Agulhas Current over and that multi-year periods, in addition to background fluctuations prevail over long-term trends (Elipot and Beal 2018). International monitoring efforts such as the ASCA line (Morris et al. 2017) could resolve ambiguities arising from the extrapolation of short-term records. Our analysis does not claim the whole Agulhas Current is strengthening, only along the shelf-edge of the eastern Agulhas Bank.

Another way of placing these results in perspective is to compare trends in coastal SST with variance from the annual cycle (i), inter-annual variability (ii), and intra-seasonal fluctuations (iii). The index-area standard deviations are: 2.5°C (i), 0.7°C (ii), and 0.9°C (iii) respectively, compared with a 35-yr decline in coastal SST of -2.4°C. Applying linear regression to coastal SST data with and without the annual cycle achieves r = -.29 vs -.76. Either way the trend is significant, not only statistically but in terms of environmental impact.

In this study, modern reanalysis datasets have been used for mapping the marine climate trends over the southern shelf of South Africa. Cross-shelf gradients in sea temperatures, latent heat flux, currents and upwelling are apparent in the satellite era. SST in the offshore zone is~~are~~ warming (.05°C/yr) since 1980 and there is a trend toward easterly winds, mainly in summer (U = -.015 m s^{-1}/yr). The shelf-edge Agulhas Current is accelerating (U = -.006 m s^{-1} /yr) in longitudes 21-28E (cf. Fig 2c) partly due to large scale winds over the southwest Indian Ocean (Backeberg et al. 2012) that align with the local forcing seen here. The faster current and 'following' wind induces coastal uplift (Leber et al. 2017) and cooling (-.03°C/yr). As the sub-tropical ridge is drawn poleward, the cross-shore gradient steepens (cf. Fig A1). Cooler near-shore sea temperatures correspond with ~~contribute to~~ atmospheric subsidence, drying trends (-.005 mm day^{-1}/yr) and vegetation warming (.1°C/yr). Similar trends in local air-sea interactions are attributed to more frequent wind-driven coastal upwelling and easterly winds (cf. Fig 3a) similar to ~~in~~ Malan et al. (2019). Coupled ensemble projections from the Hadley and European models indicate that the shift toward drier weather, easterly winds, coastal upwelling and a locally faster Agulhas Current may be sustained through the 21st century (cf. Fig 6c), as a local response to the poleward shift of the sub-tropical ridge. Some of the environmental changes could ~~benefit marine productivity and~~ create opportunities for resource adaptation (Jury 2019) and ~~. Likely socio-economic consequences include an enhanced fishery that could~~ spark interest in aquaculture and ecotourism.

While the shelf may benefit, terrestrial water resources could be headed towards greater stress. Although the hydrology is transitionally located between a drying west and moistening east, the Sundays River sees inter-basin transfers while the Gamtoos River depends on agricultural 're-cycling'. In both cases reduced runoff linked to rainfall could inhibit freshwater fluxes to the coastal ocean (cf. Fig 6b).

Parallel work on this geographic niche (Jury 2019, Jury and Goschen 2020) is on-going and further studies will: i) compare observation and reanalysis trends, ii) consider how changing satellite technology represents shelf dynamics, iii) quantify wind- vs current-driven upwelling, and iv) analyze coupled models capable of detecting sharp coastal gradients.

Acknowledgements

SAPSE funding support from South Africa is acknowledged. Reanalysis and projection ~~Most~~ data derive from websites of the IRI Climate Library, KNMI Climate Explorer and Univ Hawaii AP-DRC.

References

Arblaster JM, Meehl G, Karoly D. 2011. Future climate change in the southern hemisphere: Competing effects of ozone and greenhouse gases, *Geophysical Research Letters* 38: L02701, doi10.1029/2010GL045384.

Backeberg B, Penven P, Rouault M. 2012. Impact of intensified Indian Ocean winds on mesoscale variability in the Agulhas system. *Nature Clim Change* 2: 608–612.

Balmaseda MA, Mogensena K, Weaver AT. 2013. Evaluation of the ECMWF ocean reanalysis system ORAS4, *Quarterly Journal of the Royal Meteorology Society* 139: 1132–1161.

Carton JA, Chepurin GA, Chen L. 2018. SODA-3: A new ocean climate reanalysis. *Journal of Climate* 31: 6967–6983.

Chaudhuri AH, Ponte RM, Forget G, Heimbach P. 2013. A comparison of atmospheric reanalysis surface products over the ocean and implications for uncertainties in air–sea boundary forcing. *Journal of Climate* 26: 153–170.

Collins WJ, 17 co-authors. 2011. Development and evaluation of an Earth-System model – HadGEM2. *Geoscience Model Development* 4: 1051–1075.

Decker M, Brunke MA, Wang Z, Sakaguchi K, Zeng X and Bosilovich MG. 2012. Evaluation of the reanalysis products from GSFC, NCEP, and ECMWF using flux tower observations. *Journal of Climate* 25: 1916–1944.

Dee DP, 35 co-authors, 2011. The ERA-interim reanalysis: configuration and performance of the data assimilation system. *Quarterly Journal of the Royal Meteorological Society* 137: 553–597.

Dieppois B, Rouault M & New M. 2015. The impact of ENSO on Southern African rainfall in CMIP5 ocean atmosphere coupled climate models. *Climate Dynamics* 45: 2425–2442.

Dlomo X. 2014. Sea surface temperature trends around Southern Africa. *MSc thesis*, Univ. Cape Town, 61 pp. < open.uct.ac.za/bitstream/handle/11427/12828/thesis_sci_2014_dlomo_x.pdf >

Doblas-Reyes FJ, 17 co-authors. 2018. Using EC-Earth for climate prediction research, *ECMWF newsletter* 154, < www.ecmwf.int/en/newsletter/154/meteorology/ >

Durgadoo JV, Loveday BR, Reason CJ, Penven P, Biastoch A. 2013. Agulhas leakage predominantly responds to the Southern Hemisphere westerlies. *Journal of Physical Oceanography* 43: 2113–2131.

Elipot S, Beal LM. 2015. Characteristics, energetics and origins of Agulhas Current meanders and their limited influence on ring shedding. *Journal of Physical Oceanography* 45: 2294–2314.

Formatiert: Schriftart: Kursiv

Elipot S, Beal LM. 2018. Observed Agulhas Current sensitivity to interannual and long-term trend atmospheric forcings. *Journal of Climate* 31: 3077–3098.

Funk CC, Peterson PJ, Landsfeld MF, Pedreros DH, Verdin JP, Rowland JD, Romero BE, Husak GJ, Michaelsen JC and Verdin AP. 2014. A quasi-global precipitation time series for drought monitoring. *US Geological Survey Data Series* 832: 1–4, doi10.110.3133/ds832.

Formatiert: Schriftart: Kursiv

Gelaro R, 30 co-authors. 2017. The Modern-Era Retrospective Analysis for Research and Applications, version 2 (MERRA-2). *Journal of Climate* 30: 5419–5454.

Goschen WS, Schumann EH. 1990. Agulhas Current variability and inshore structures off the Cape Province, South Africa. *Journal of Geophysical Research* 95: 667–678.

Goschen WS, Bornman TG, Deyzel SHP, Schumann EH. 2015. Coastal upwelling on the far eastern Agulhas Bank associated with large meanders in the Agulhas Current. *Continental Shelf Research* 101: 34–46.

Hamrud M, Bonavita M, Isaksen L. 2015. Kalman filter and hybrid-gain ensemble data assimilation. Part I: EnKF implementation. *Monthly Weather Review* 143: 4847–4864.

Hutchinson K, Beal LM, Penven P, Ansorge I, Hermes J. 2018. Seasonal phasing of Agulhas Current transport tied to a baroclinic adjustment of near-field winds. *Journal of Geophysical Research*

Oceans 123: 7067–7083.

Jury MR, MacArthur C, Reason C. 1990. Observations of trapped waves in the atmosphere and ocean along the coast of southern Africa. *South African Geographical Journal* 72: 33–46.

Jury MR. 2013. Climate trends in southern Africa. *South African Journal of Science* 109: 53–63.

Jury MR. 2015. Passive suppression of South African rainfall by the Agulhas Current, *Earth Interactions* 19: 1–14.

~~Jury MR. 2018. Puerto Rico sea level trend in regional context, *Journal of Ocean and Coastal Management* 163: 478–484.~~

~~Jury MR. 2019. Meteorological controls on big waves south of Africa, *Regional Studies in Marine Science* 27: 100538.~~

Jury MR. 2019. Environmental controls on marine productivity near Cape St Francis, South Africa, *EGU Ocean Science*, doi.org/10.5194/os-2019-55.

Jury MR. 2020. Slowing of Caribbean through-flow, *Deep Sea Research* 2: 168, doi10.1016/j.dsr2.2019.104682.

Jury MR. and Goschen W.S. 2020. Physical ocean-atmosphere variability over the shelf of South Africa from reanalysis products. *Continental Shelf Research*, (in press).

Kennedy AD, Dong X, Xi B, Xie S, Zhang Y, Chen J. 2011. A comparison of MERRA and NARR reanalyses with the DOE ARM SGP data. *Journal of Climate* 24: 4541–4557.

Kruger AC, Shongwe S. 2004. Temperature trends in South Africa: 1960–2003. *International Journal of Climatology* 24: 1929–1945.

Kruger AC, Nxumalo MP. 2017. Historical rainfall trends in South Africa: 1921–2015, *WaterSA* 43: 285–297.

Leber GM, Beal LM and Elipot S. 2017: Wind and current forcing combine to drive strong upwelling in the Agulhas Current. *Journal of Physical Oceanography*, 47, 123–134,

Lee H-T, Gruber A, Ellingson RG, Laszlo I. 2007. Development of the HIRS outgoing longwave radiation climate dataset. *Journal of Atmospheric and Oceanic Technology* 24: 2029–2047.

Lutjeharms JRE. 2006. *The Agulhas Current*. Springer, Berlin: 329 pp.

Lutjeharms JRE, Cooper J, Roberts MJ. 2000. Upwelling at the inshore edge of the Agulhas Current. *Continental Shelf Research* 20: 737–761.

MacKeller N, New M, Jack C. 2014. Observed and modelled trends in rainfall and temperature for South Africa: 1960–2010. *South African Journal of Science* 110: 1–13.

Malan N, Backeberg B, Biastoch A, Durgadoo JV, Samuelsen A, Reason C, Hermes J. 2018. Agulhas Current Meanders facilitate shelf - slope exchange on the Eastern Agulhas Bank. *Journal of Geophysical Research Oceans* 123: 4762–4778.

Malan NC, Durgadoo JV, Biastoch A, Reason CJ, Hermes, JC. 2019. Multidecadal wind variability drives temperature shifts on the Agulhas Bank. *Journal of Geophysical Research Oceans* 124: 3021– 3035.

Mather AA, Garland GG, Stretch DD. 2009. Southern African sea levels: corrections, influences and trends, *African Journal of Marine Science* 31: 145–156.

Morishima W, Akasaka I. 2010. Seasonal trends of rainfall and surface temperature over Southern Africa. *African Study Monographs* 40: 67–76.

Morris T, Hermes J, Beal L, du Plessis M, Rae CD, Gulekana M, Lamont T, Speich S, Roberts M, Ansorge IJ. 2017. The importance of monitoring the Greater Agulhas Current and its inter-ocean exchanges using large mooring arrays. *South African Journal of Science* 113: 1–7.

Nkwinkwa N, Rouault M, Johannessen JA. 2019. Latent heat flux in the Agulhas Current. *MDPI Remote Sensing* 11: 1576.

Pattrick P, Strydom NA, Goschen WS. 2013. Shallow-water, nearshore current dynamics in Algoa Bay, South Africa, with notes on the implications for larval fish dispersal. *African Journal of Marine Science* 35: 269–282.

Philippon N, Rouault M, Richard Y, Favre A. 2012. The influence of ENSO on winter rainfall in South Africa. *International Journal of Climatology* 32: 2333–2347.

Poli P, 14 co-authors. 2016. ERA-20C: An atmospheric reanalysis of the Twentieth Century. *Journal of Climate* 29: 4083–4097.

Reynolds RW, Smith TM, Liu C, Chelton DB, Casey KS, Schlax MG. 2007. Daily high-resolution blended analyses for sea surface temperature. *Journal of Climate* 20: 5473–5496.

Roberts MJ. 2010. Coastal currents and temperatures along the eastern region of Algoa Bay, South Africa, with implications for transport and shelf-bay water exchange. *African Journal of Marine*

Formatiert: Schriftart: Kursiv

Science 32: 145–161.

Rouault M, Penven P, Pohl B. 2009. Warming in the Agulhas Current system since the 1980s. *Geophysical Research Letters*, 36: L12602.

Rouault M, Pohl B, Penven P. 2010. Coastal oceanic climate change and variability from 1982 to 2009 around South Africa. *African Journal of Marine Science* 32: 237–246.

Rouault MJ, Penven P. 2011. New perspectives on Natal Pulses from satellite observations. *Journal of Geophysical Research Oceans* 116: 1–14.

Saha S, 51 co-authors. 2010. The NCEP Coupled Forecast System reanalysis. *Bulletin of the American Meteorological Society* 91: 1015–1057.

Scharler UM, Baird D. 2005. The filtering capacity of selected Eastern Cape estuaries, South Africa. *WaterSA* 31: 483–490.

Schlegel RW, Smit AJ. 2016. Climate change in coastal waters: time series properties affecting trend estimation. *Journal of Climate* 29: 9113–9124.

Schumann EH. 1999. Wind-driven mixed layer and coastal upwelling processes off the south coast of South Africa. *Journal of Marine Research* 57: 671–691.

Schumann EH, Perrins L-A, Hunter IT. 1982. Upwelling along the south coast of the Cape Province, South Africa. *South African Journal of Science* 78: 238–242.

Schumann EH, Beekman LJ. 1984. Ocean temperature structures on the Agulhas Bank. *Transactions of the Royal Society of South Africa* 45: 191–203.

Schumann EH, Brink KH. 1990. Coastal trapped waves off the coast of South Africa: generation, propagation and current structures. *Journal of Physical Oceanography* 20: 1206–1218.

Schumann EH, Martin JA. 1991. Climatological aspects of the coastal wind field at Cape Town, Port Elizxabeth and Durban. *South African Geographical Journal* 73: 48–51.

Schumann EH, Pearce MW. 1997. Freshwater inflow and estuarine variability in the Gamtoos Estuary, South Africa. *Estuaries* 20: 124–133.

Swart VP, Largier JL. 1987. Thermal structure of Agulhas Bank water, *South African Journal of Marine Science* 5: 243–252.

Tadross M, Jack C, Hewitson B. 2005. On RCM-based projections of change in southern African

Formatiert: Schriftart: Kursiv

summer climate. *Geophysical Research Letters* 32: L23713, doi:10.1029/2005GL024460.

Taylor KE, Stouffer RJ, Meehl GA. 2012. An overview of CMIP5 and the experiment design. *Bulletin of the American Meteorological Society* 93: 485–498.

Tucker CJ, Pinzon JE, Brown ME, Slayback DA, Pak EW, Mahoney R, Vermote EF, el Saleous N. 2005. An extended AVHRR 8 km NDVI dataset compatible with MODIS and SPOT vegetation data. *International Journal of Remote Sensing* 26: 4485–4498.

van Bladeren D, Zawada PK, Mahlangu D. 2007. Statistical based regional flood frequency estimation study for South Africa using systematic, historical and paleo-flood data. *Water Research Commission Report* 1260/1/70, Pretoria.

VanVuuren DP, 14 co-authors. 2011. The representative concentration pathways: an overview, *Climatic Change* 109: 5–31.

Table 1 Datasets used in the analysis, web sources are listed in acknowledgement.

ACRONYM	NAME	RESOLUTION	TIME SPAN
CFSr-2	Coupled Forecast System v2 coupled (air-land-sea) reanalysis	0.35 deg	1980-2015
CHIRP	Climate Hazards InfraRed Precipitation (via Meteosat)	0.05 deg	1981-2016
ECMWF-5	European Community Medium-range Weather Forecasts v5 coupled reanalysis	0.25 deg	1980-2016
ECMWF-20c	European Community Medium-range Weather Forecasts 20th century atmosphere reanalysis	1.0 deg	1900-2010
ECMWF-ora4	European Community Medium-range Weather Forecasts ocean reanalysis	1.0 deg	1958-2016
ECMWF-esm	European Community Medium-range Weather Forecasts coupled ensemble 21st century projections	1.2 deg	1980-2100
Hadley-esm	Hadley Centre coupled ensemble model 21st century projections for oceanography	1.5 deg	2005-2100
MERRA-2	Modern Era Reanalysis for Research and Applications v2 (NASA)	0.5 deg	1980-2015
NOAA	National Oceanic and Atmospheric Administration surface temperature and net outgoing longwave radiation	0.25 deg (SST) 1.0 deg (OLR)	1981-2016
SADCO SADW	S. Africa Data Centre Oceanogr. S.A. Dept. of Water Affairs	In-situ measurements	1950-2015 1980-2016
SODA-3	Simple Ocean Data Assimilation Reanalysis v3	0.5 deg	1980-2015

Figures

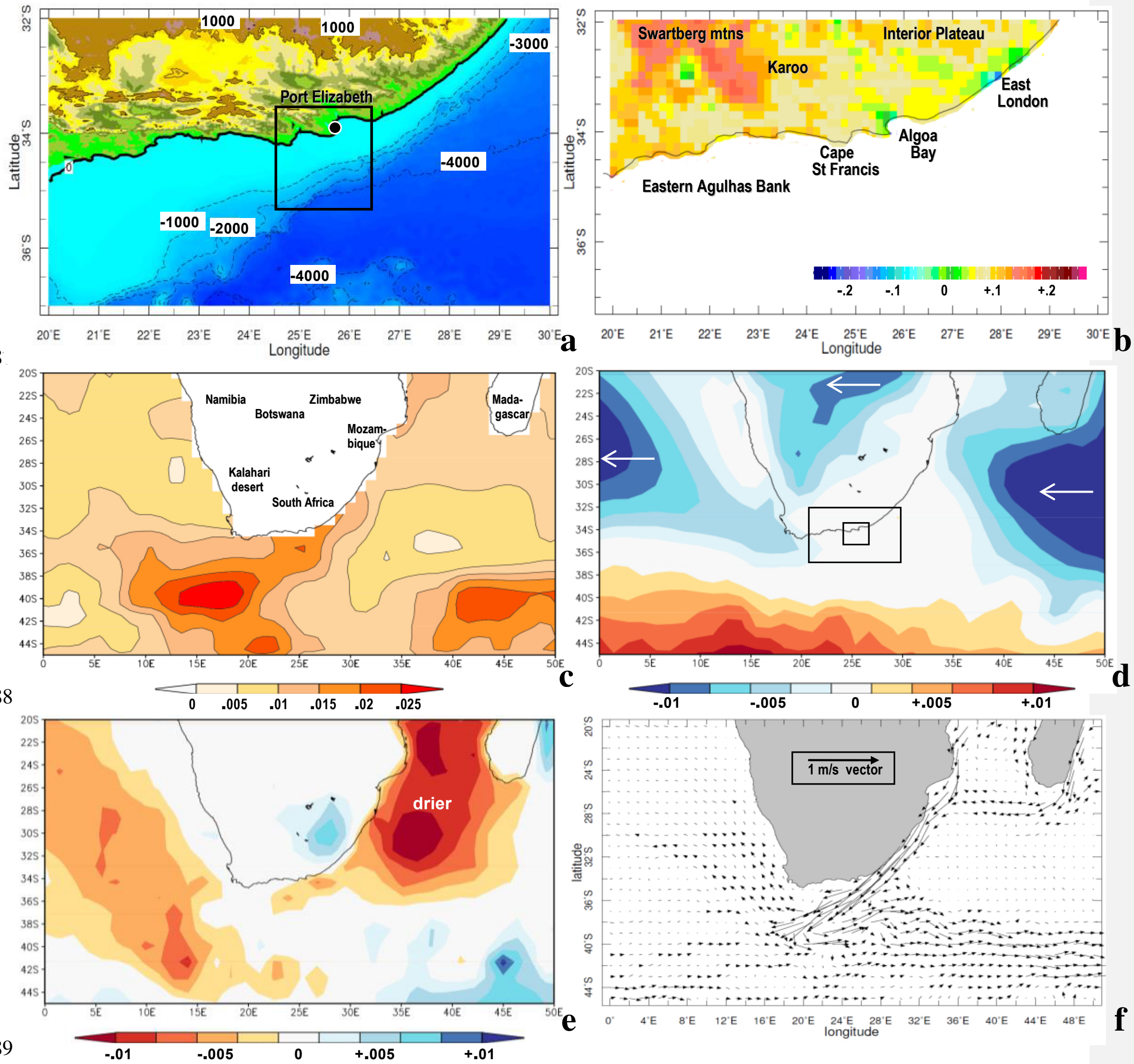

Figure 1 (a) Topography / bathymetry of the study area with index for temporal analyses (box) and Port Elizabeth (dot). (b) Linear trend in annual NOAA vegetation temperature (C/yr 1981-2016). Large-scale trends in annual: (c) Hadley SST (C/yr 1900-2016), (d) ECMWF-20c zonal wind (m s^{-1}/yr 1900-2010), with inner study domains, and (e) ECMWF-20c precipitation minus evaporation trend (mm day^{-1}/yr). (f) SODA3 mean 1-100 m currents (vector, with scale inset). Geographical labels are given in (b,c).

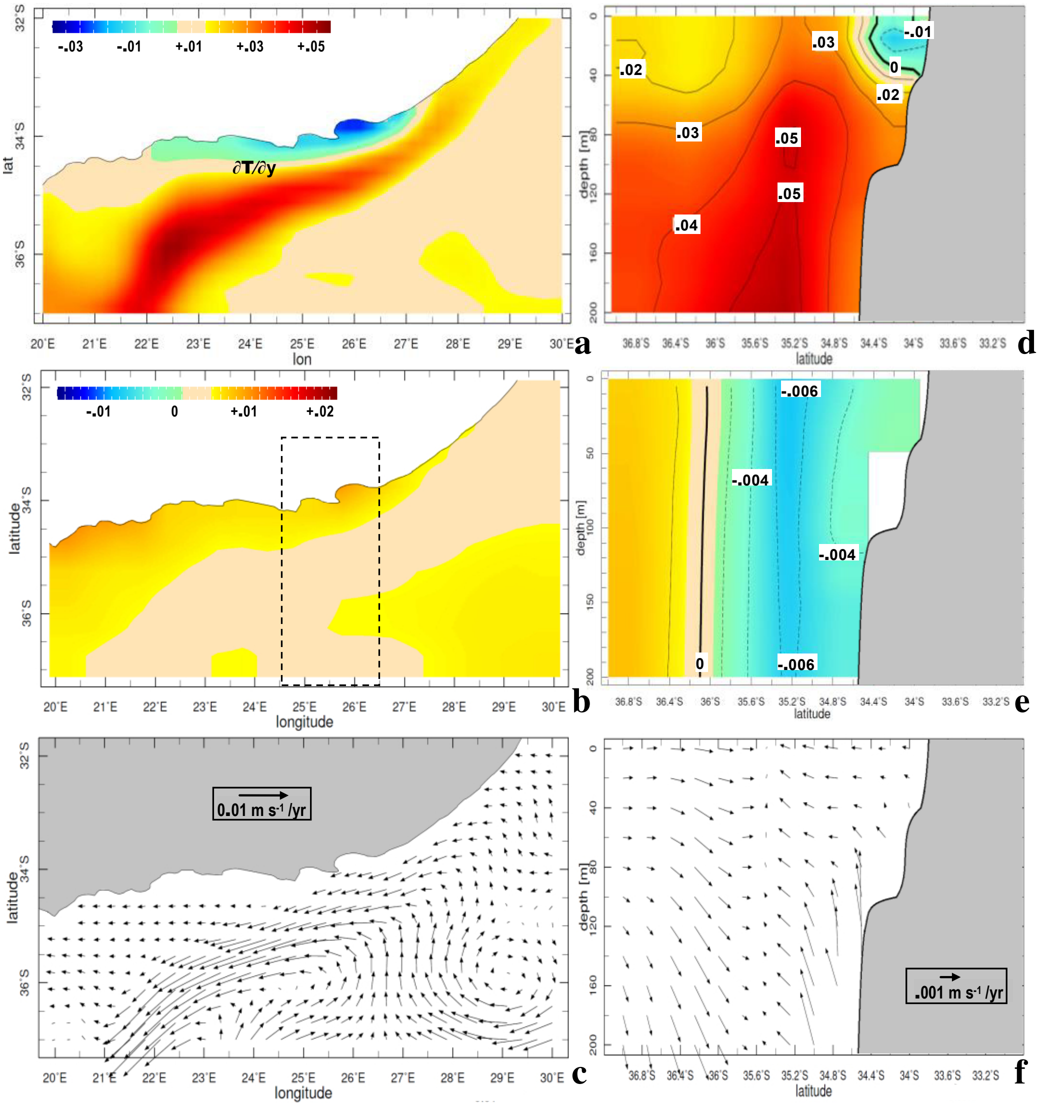

Figure 2 Regional trends in annual (a) NOAA sea surface temperature (C/yr 1981-2016); SODA-3 1980-2015: (b) 1-10 m salinity (ppt/yr) with section denoted, and (c) 1-50 m currents (m s^{-1}/yr vector); and depth section averaged 24.5-26.5E of (d) sea temperature (C/yr), (e) zonal current (m s^{-1}/yr), and (f) meridional circulation (m s^{-1}/yr vector, with W exaggerated). Vector scales are inset.

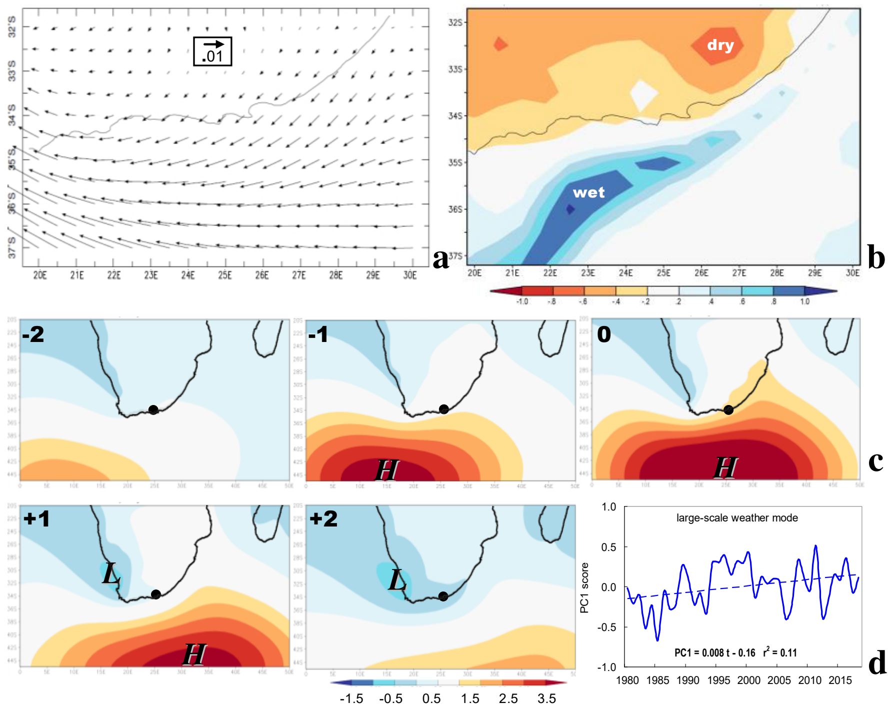

Figure 3 (a) Regional trend in annual CFSr-2 surface wind (m s^{-1}/yr vector, 1980-2015) and (b) latent heat flux (W m^{-2}/yr). (c) Large-scale summer weather mode-1 in daily ECMWF sea level air pressure principal component loading pattern at lags -2, -1, 0, +1, +2 days (hPa) and (d) time score. PC1 represents 38% of variance, dot in (c) is the study area, inset in (d) is the slope and fit of the linear regression.

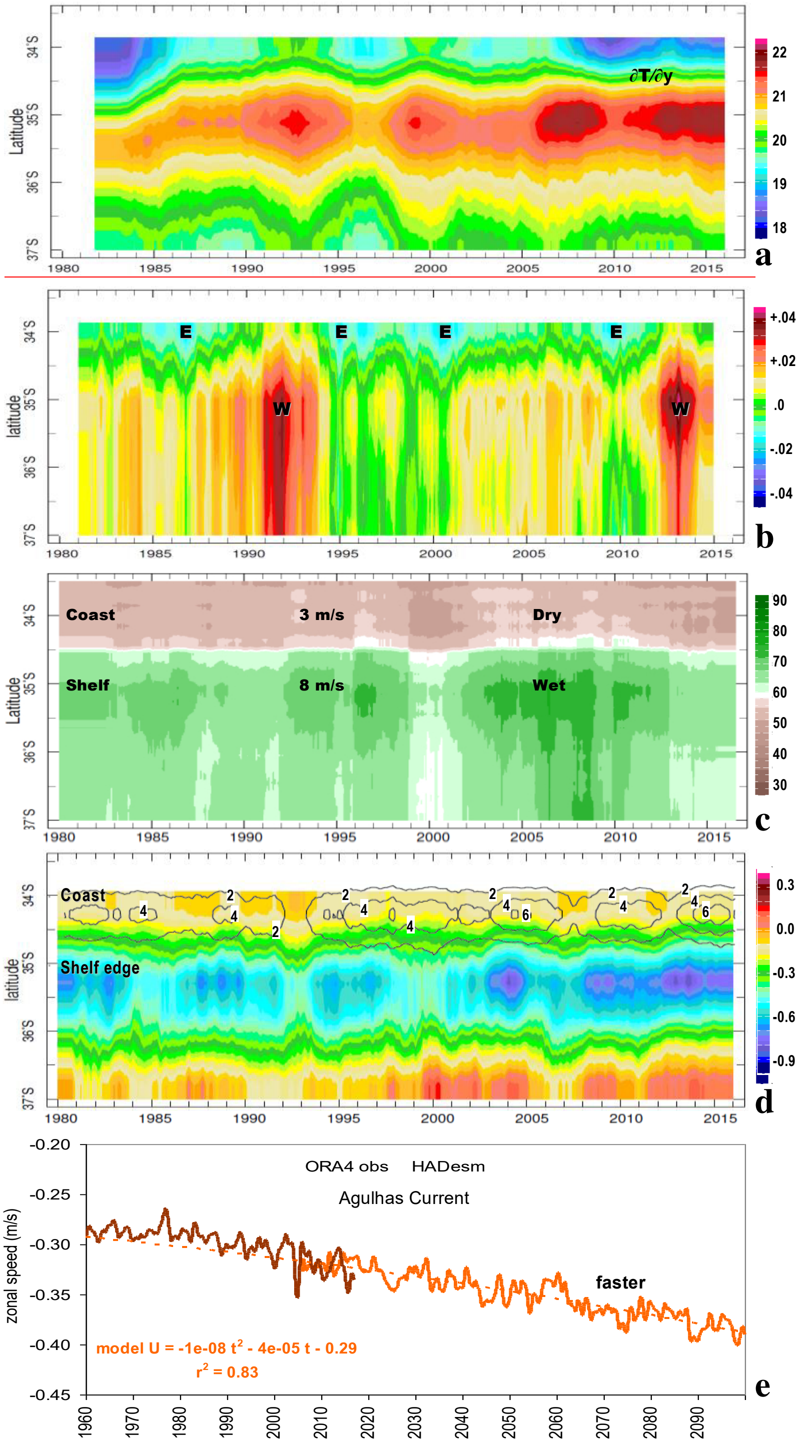

Figure 4 Hovmoller plots of 18-month filtered variables avg. 24.5-26.5E: (a) NOAA SST (C), (b) zonal wind stress (N/m^2), (c) CHIRP rainfall (mm/month), (d) SODA-3 1-50 m zonal current (shaded m/s) and 1-200 m upward motion (contour m/day). (e) Index-area time series of observed and projected 1-50 m zonal current. 'Coast' and 'Shelf' climates and average wind speeds are labelled in (c).

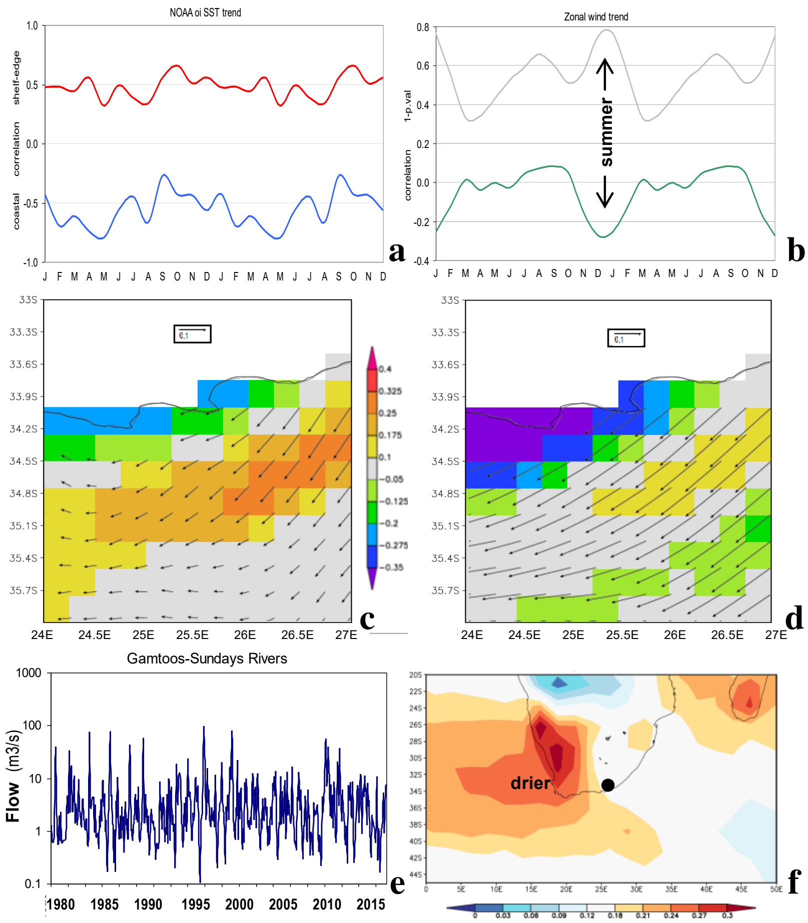

Figure 5 Analysis of monthly index-area trends for (a) coastal and shelf-edge SST, and (b) zonal wind and its significance (1-p value), with 35 degrees of freedom. Regression of (c) annual and (d) summer NOAA SST (shading °C) and SODA-3 surface wind (vector, scale inset m/s) with the SOI index 1981-2016 (units are per SOI fraction). (e) Observed discharge of the combined Gamtoos and Sundays Rivers. (f) Trend of NOAA net outgoing longwave radiation as a proxy for cloudiness (W m^{-2}/yr 1979-2017) with dot showing river gauges.

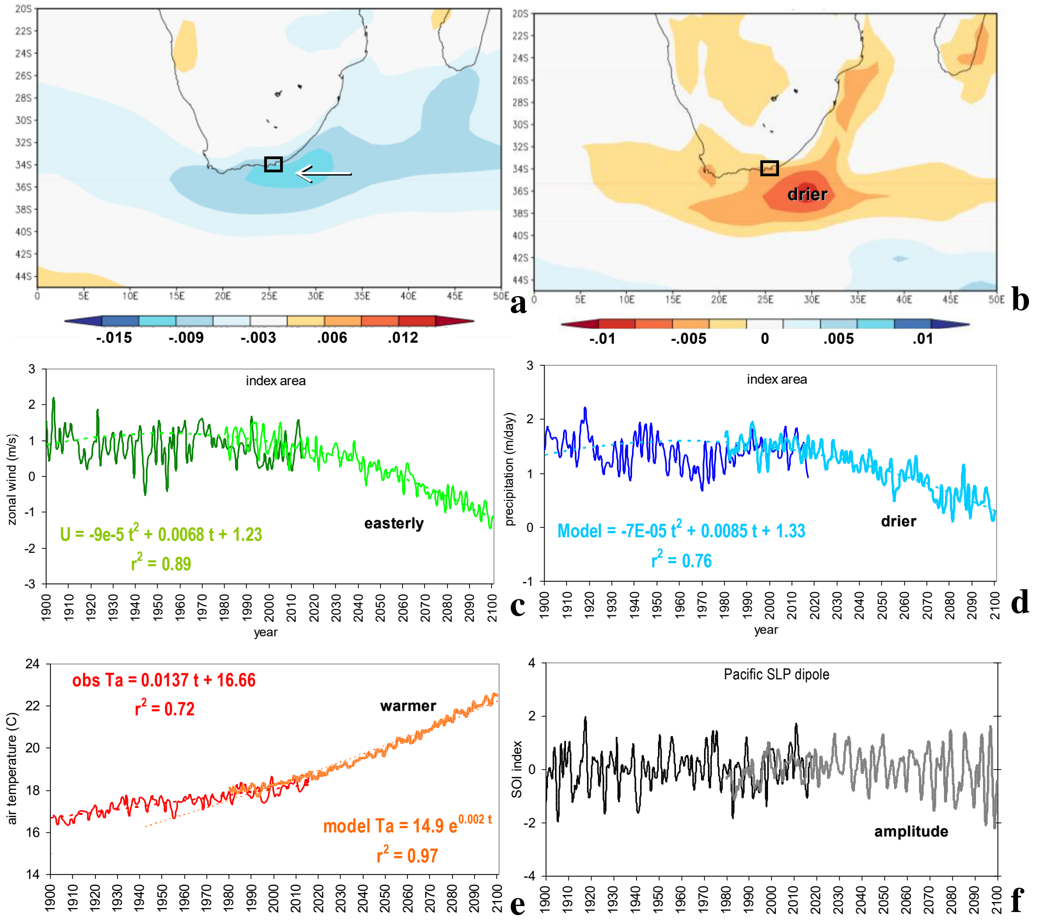

Figure 6 EC-esm projected trend maps 1980-2100: (a) zonal wind (m s^{-1}/yr), (b) precipitation (mm day^{-1}/yr). Temporal record of index area ECMWF-20C reanalysis 1900-2010 and EC-esm projected 1980-2100: (c) zonal wind, (d) precipitation, and (e) air temperature. (f) Observed and model projected Pacific southern oscillation index (east-west SLP EOF mode). Best-fit trends are given; time series are composed of annual averages.

Appendix

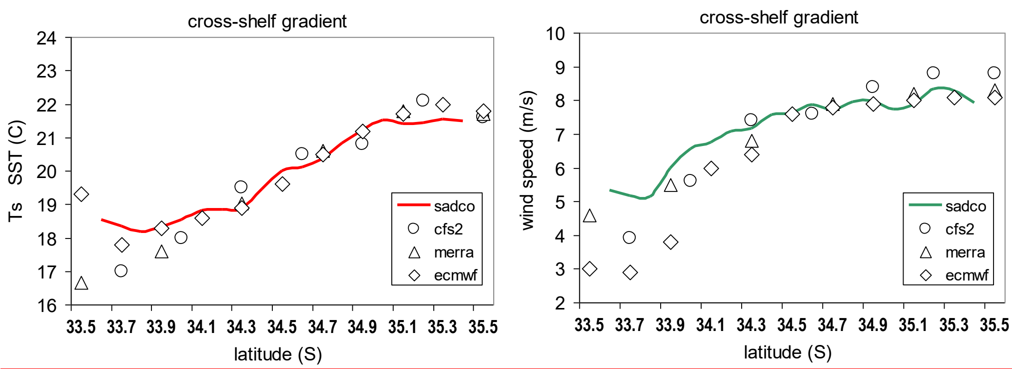

Fig A1 SADCO ship data~~,~~ averageds per ~~in each~~ 0.1 latitude bin over 24.5-26.5E longitude 1950-2015~~; left axis and dashed line refer to standard deviation;~~ (line) and comparativ~~eison with~~ satellite era ~~0.3~~ reanaly-sis~~binned CFSr2 (left) and ECMWF~~ (dots).

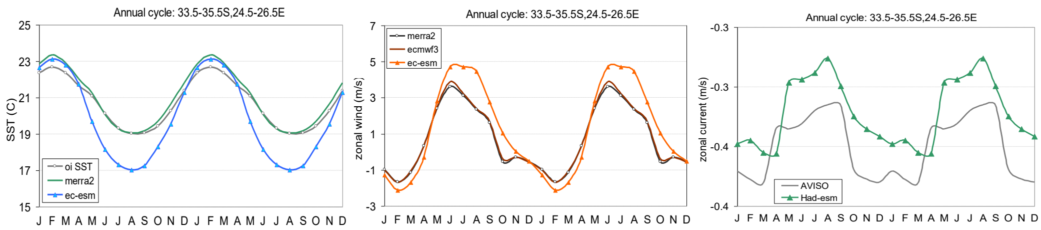

Fig A2 Annual cycles averaged over the index area; comparing model SST, surface zonal wind (middle) and near-surface current with reference product. The model has an amplified annual cycle that is cooler and more westerly in winter. Currents show summer / winter regimes with model slightly weaker and delayed.

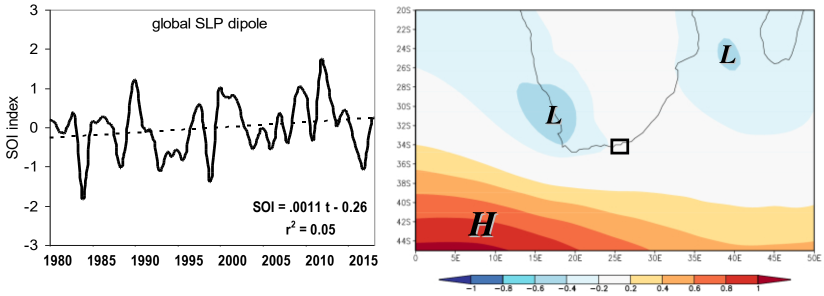

Fig A3 Graph of 18-month filtered southern oscillation index and its trend in the satellite era, and regression of Dec-Feb SOI onto regional sea level air pressure (hPa), with boxed index area.